

A LINK BETWEEN X-RAY EMISSION LINES AND RADIO JETS IN 4U 1630–47?

JOSEPH NEILSEN^{1,2,9}, MICKAËL CORIAT³, ROB FENDER⁴, JULIA C. LEE⁵, GABRIELE PONTI⁶, ANASTASIOS K. TZIOUMIS⁷,
 PHILIP G. EDWARDS⁷, JESS W. BRODERICK⁸

Draft version February 24, 2014

ABSTRACT

Recently, Díaz Trigo et al. reported an *XMM-Newton* detection of relativistically Doppler-shifted emission lines associated with steep-spectrum radio emission in the stellar-mass black hole candidate 4U 1630–47 during its 2012 outburst. They interpreted these lines as indicative of a baryonic jet launched by the accretion disk. Here we present a search for the same lines earlier in the same outburst using high-resolution X-ray spectra from the *Chandra* High-Energy Transmission Grating Spectrometer. While our observations (eight months prior to the *XMM-Newton* campaign) also coincide with detections of steep spectrum radio emission by the Australia Telescope Compact Array, we find no evidence for any relativistic X-ray emission lines. Indeed, despite $\sim 5\times$ brighter radio emission, our *Chandra* spectra allow us to place an upper limit on the flux in the blueshifted Fe XXVI line that is $\gtrsim 20\times$ weaker than the line observed by Díaz Trigo et al. We explore several scenarios that could explain our differing results, including variations in the geometry of the jet or a mass-loading process or jet baryon content that evolves with the accretion state of the black hole. We also consider the possibility that the radio emission arises in an interaction between a jet and the nearby ISM, in which case the X-ray emission lines might be unrelated to the radio emission.

Subject headings: accretion, accretion disks — black hole physics — X-rays: individual (4U 1630–47)
 — X-rays: binaries — stars: winds, outflows — ISM: jets and outflows

1. INTRODUCTION

Collimated jets are ubiquitous in accreting systems across the mass scale, from protostars (e.g., Carrasco-González et al. 2010) to supermassive black holes in AGN at the centers of galaxy clusters (e.g., McNamara et al. 2000; Fabian et al. 2000). But the omnipresence of jets in astrophysical systems raises important questions. Are all these jets produced by the same processes? Since one of the canonical jet formation mechanisms (the Blandford-Znajek, or BZ, mechanism; Blandford & Znajek 1977; Tchekhovskoy et al. 2011), involves the rotation power of a black hole, it certainly cannot operate in all systems. An alternative is the Blandford-Payne mechanism (BP; Blandford & Payne 1982), in which the requisite rotation power comes from a rotating accretion disk. As a consequence, one expects BP jets to be baryonic, since they are magnetocentrifugal outflows from a gaseous reservoir. BZ jets, on the other hand, might be electromagnetically dominated.

In this context, it is particularly interesting that accreting stellar-mass black holes appear to produce two

different kinds of jets (steady and transient; for reviews see Fender et al. 2004, 2009). Observationally, it remains unclear whether these two types of jets correspond to the two mechanisms described above; a suggested association between the transient jets and the BZ mechanism has lately been the subject of significant debate (Fender et al. 2010; Narayan & McClintock 2012; Steiner et al. 2013; Russell et al. 2013; King et al. 2013a). The formation of steady jets is no less significant, as it has been suggested (Neilsen & Lee 2009; see also Miller et al. 2008; Neilsen et al. 2011; Neilsen & Homan 2012; King et al. 2013b and references therein) that ionized accretion disk winds may be able to quench steady jets. Different processes may launch astrophysical jets at different scales or under different conditions, but because a jet’s energy requirements are sensitive to its baryon content (see, e.g., Fender et al. 1999; Gallo et al. 2005; Heinz 2006; Punsly & Rodriguez 2013), these considerations have broad and concrete implications for radio-mode feedback from accreting systems.

Recently, Díaz Trigo et al. (2013; hereafter DT13) reported a detection of relativistically-blueshifted emission lines associated with radio emission in the stellar-mass black hole candidate 4U 1630–47, a well-known recurrent transient (Jones et al. 1976; Kuulkers et al. 1997; Tomsick et al. 2005) that went into outburst in December 2011 (Neilsen 2013). DT13 reported on two observations of the source with *XMM-Newton* and the Australia Telescope Compact Array (ATCA) in 2012 September. In their first observation (September 10–12), they found a featureless X-ray spectrum and no radio emission. In their second observation (September 28–29), however, they discovered optically thin radio emission and X-ray emission lines at energies that do not correspond to strong lines from abundant elements. They argued that the emission lines originated in a relativistic jet with

¹ Department of Astronomy, Boston University, Boston, MA 02215, USA; neilsenj@bu.edu

² MIT Kavli Institute for Astrophysics and Space Research, Cambridge, MA 02138, USA

³ Department of Astronomy, University of Cape Town, Private Bag X3, Rondebosch 7701, South Africa

⁴ Department of Physics, Brasenose College, University of Oxford, Oxford, OX1 3RH, UK

⁵ Harvard-Smithsonian Center for Astrophysics, Cambridge, MA 02138

⁶ Max Planck Institute für Extraterrestrische Physik, 85748, Garching, Germany

⁷ CSIRO Astronomy and Space Science, Australia Telescope National Facility, PO Box 76, Epping, NSW 1710, Australia

⁸ School of Physics and Astronomy, University of Southampton, Highfield, Southampton, SO17 1BJ, UK

⁹ Einstein Fellow

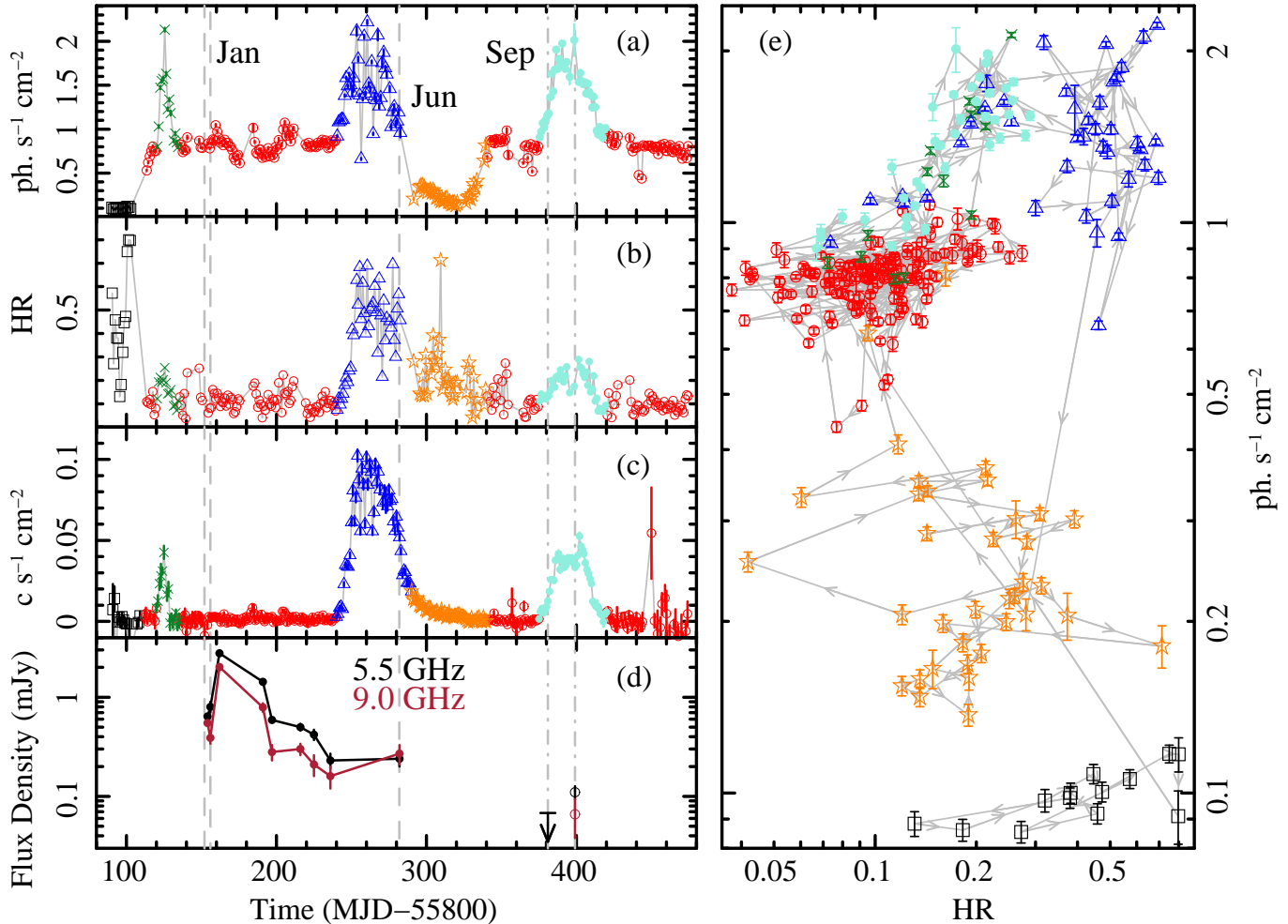


FIG. 1.— Monitoring of the 2012 outburst of 4U 1630–47. (a) 2–20 keV MAXI light curve. (b) MAXI hardness ratio (10–20/2–4 keV). (c) 15–50 keV *Swift*/BAT light curve. (d) 5.5 GHz and 9 GHz radio fluxes as measured by ATCA by us and DT13. Dashed and dash-dotted vertical lines indicate the times of the *Chandra* and *XMM* observations, respectively. (e) MAXI hardness-intensity diagram. The colors/symbols are rough indicators of the accretion state.

a speed of $\sim 0.66c$, where c is the speed of light. In their interpretation, the lines corresponded to red- and blueshifted Fe xxvi Ly α and blueshifted Ni xxvii He α .

In this paper, we report on ATCA and *Chandra* High-Energy Transmission Grating Spectrometer (HETGS; Canizares et al. 2005) observations of the same outburst of 4U 1630–47. Although we detect radio emission at levels brighter than those reported in DT13, we do not detect the X-ray emission lines seen later in the outburst. Indeed, our *Chandra* spectra place tight upper limits on such features, and we can conclusively say that radio emission is not universally associated with relativistically Doppler-shifted emission lines in 4U 1630–47. While our results do not and cannot directly address the argument for the presence of baryons in the 2012 September jet in 4U 1630–47, we highlight the necessity of a complex relationship between X-ray and radio emission, considering not only the possibility of undetected baryons in the January and June jets or baryonic jets confined to a particular accretion state, but also an alternative scenario in which the radio emission arises in a jet-ISM interaction and could be decoupled from the X-ray emission.

2. OBSERVATIONS AND DATA REDUCTION

2.1. *Chandra* HETGS

After the peak of the outburst around 2012 January 1, we triggered our *Chandra* HETGS campaign, observing the source for ~ 29 ks four times: January 17 (4:23:43 UT), January 20 (23:43:52 UT), January 26 (13:00:35 UT), and January 30 (8:48:41 UT). The data were taken in Graded mode with a grey filter over the zeroth order to reduce the risk of telemetry saturation from the bright source. We also obtained a 19 ks HETGS DDT in Continuous-Clocking (CC) mode (2012 June 3 22:19:16 UT) when 4U 1630–47 entered an active state. We show the MAXI/*Swift* outburst light curves and MAXI hardness-intensity diagram in Figure 1. We reduce the *Chandra* data with standard CIAO data reduction tools to create first-order High-Energy Grating (HEG) spectra and response files. Performing all our analysis within the Interactive Spectral Interpretation System (ISIS; Houck & Denicola 2000), we restrict our attention to the 1.7–9 keV band.

2.2. ATCA

We also triggered an ATCA monitoring campaign at 5.5 and 9 GHz, observing the source at 10 epochs between 2012 January 28 and June 4. The observations were

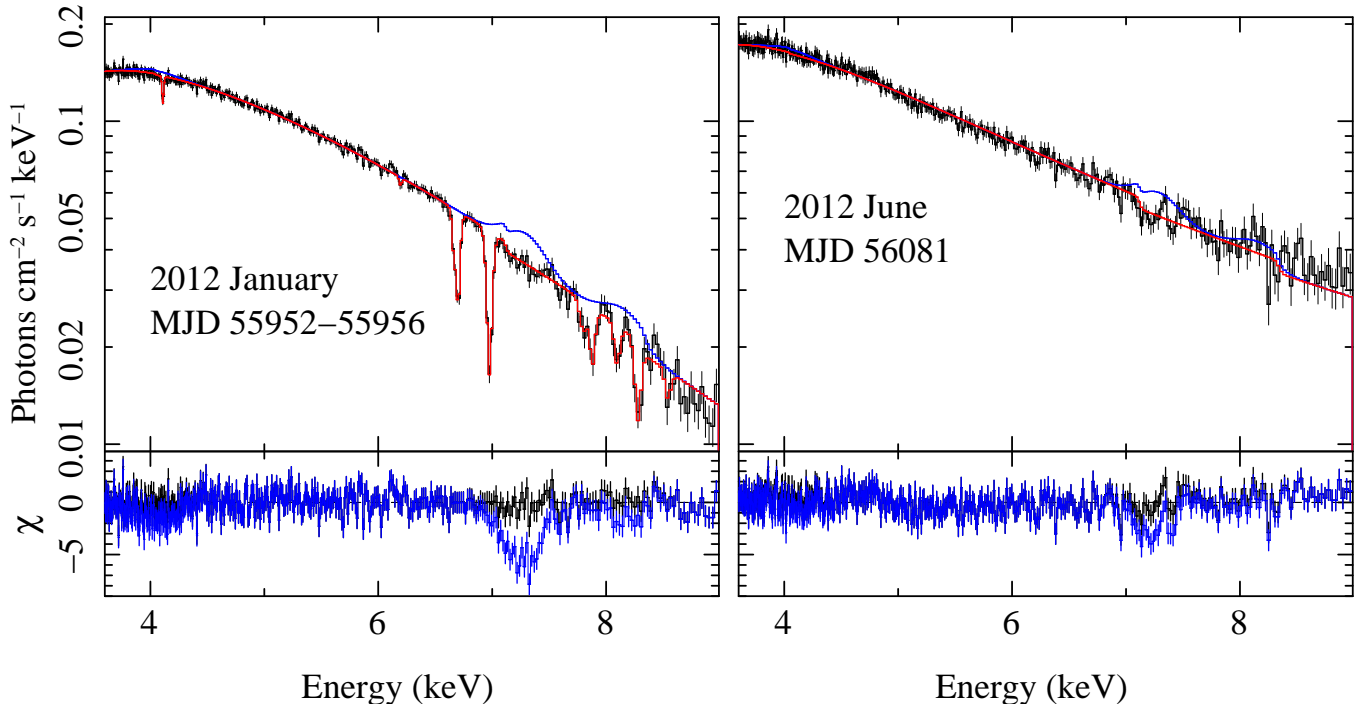


FIG. 2.— *Chandra* HETGS spectrum of 4U 1630–47 (black) from January (left) and June (right). In red, we show our best fit models. In blue, we plot the sum of the continuum emission and the relativistic lines seen by DT13. In the bottom panels are the residuals relative to our best fit; the non-detection of the relativistic lines is highly significant. See text for details.

conducted with the Compact Array Broadband Backend (CABB; Wilson et al. 2011) with the array in a number of configurations ranging from H168 (compact) to 6A (extended). Each frequency band was composed of 2048 1-MHz channels. We used PKS1934–638 for absolute flux and bandpass calibration, and J1600–48 to calibrate the antenna gains as a function of time. Flagging, calibration and imaging were carried out with the Multi-channel Image Reconstruction, Image Analysis and Display (MIRIAD) software (Sault et al. 1995). Note that the visibilities from the shortest baselines were excluded from the imaging step to avoid flux contamination from an extended source very close to 4U 1630–47.

We measured flux densities by fitting a point source in the image plane, and we achieve a significant detection of 4U 1630–47 at 5.5 and 9 GHz in every observation with useful data. The resulting ATCA light curves are plotted in the bottom panel of Figure 1 and appear to show an optically thin flare that lasts ~ 50 days and then fades slowly as the spectrum flattens.

3. RESULTS

During their second observation of 4U 1630–47 (MJD 56181), DT13 reported radio fluxes of 110 ± 17 and 66 ± 28 μJy at 5.5 GHz and 9 GHz, respectively. In order to perform the most robust comparison, we focus here on the *Chandra* observations with contemporaneous ATCA detections of optically thin radio emission (i.e., January 26 and 30, MJD 55952/55956). The ATCA pointings on January 28 and 30 have 5.5 GHz/9 GHz fluxes of 640 ± 30 μJy / 550 ± 30 μJy and 800 ± 100 μJy / 390 ± 50 μJy , respectively. For completeness, we also consider our June 3–4 (MJD 56081) *Chandra*/ATCA campaign (fluxes of 240 ± 40 μJy and 270 ± 60 μJy , respectively).

3.1. 2012 January

The most notable feature of our January *Chandra* spectra is a series of deep, blueshifted ($v \sim 200–500$ km s^{-1}), narrow absorption lines indicative of a highly-ionized accretion disk wind (including Ca XX, Fe XXV He $\alpha/\beta/\gamma/\delta$, Fe XXVI Ly α/β , Ni XXVII He α , and Ni XXVIII Ly α ; see Figure 2). Its presence is consistent with the picture put forward in Ponti et al. (2012; see also Neilsen & Homan 2012; Neilsen 2013). *NuSTAR* also detected a wind a month later (King et al. 2014). For our purposes, the wind is a confounding factor in the search for the emission lines detected by DT13; we will discuss its properties in detail in a forthcoming paper (Neilsen et al., in preparation). Here, we focus on the X-ray continuum and a search for Doppler-shifted emission lines.

We model the combined spectrum of the *Chandra* observations as a pure disk blackbody (`ezdiskbb`; Zimmerman et al. 2005) modified by interstellar absorption (`TBnew`, using Wilms et al. 2000 abundances and Verner et al. 1996 cross-sections), dust scattering (`dustscat`; Baganoff et al. 2003), and 17 narrow absorption lines. We tie the dust optical depth τ to N_{H} via the relationship $\tau = 0.324 \times 10^{-22} \text{ cm}^2 N_{\text{H}}$ (see Nowak et al. 2012 for more details on this scaling). We also allow the interstellar abundances of Si, S, and Ni to vary, and we use the model `simple_gpile2` to account for photon pileup (Davis 2001). All errors quoted below are 90% confidence limits for a single parameter.

Our best fit column density, $N_{\text{H}} = 9.4^{+0.5}_{-1.1} \times 10^{22} \text{ cm}^{-2}$, is consistent with the value reported by DT13, but the disk in our observations is both cooler and fainter than in DT13’s observations, even when accounting for the differences in our disk model (Zimmerman et al. 2005). For reference, in their second observation DT13 measured a

TABLE 1
DOPPLER-SHIFTED EMISSION LINES IN 4U 1630–47

Line	Jan.			Jun.			F_{DT13}	W_{DT13} (eV)
	F_8	E_{obs} (keV)	W_0 (eV)	F_8	E_{obs} (keV)	W_0 (eV)		
Fe _{red}	< 0.3	4.04 ^a	< 2	4 ± 1^b	$3.94^{+0.06}_{-0.0p}$ ^a	18 ± 5^b	3.0 ± 1.4	8 ± 4
Fe _{blue}	< 0.3	7.28 ^a	< 6	< 1.3	7.28 ^a	< 18	6.2 ± 1	37 ± 9
Ni _{blue}	< 10	8.14 ^a	< 270	< 4.3	8.14 ^a	< 70	2.5 ± 1.0	18 ± 10

NOTE. — Constraints on Doppler-shifted emission lines in HETGS spectra of 4U 1630–47. F_8 is the emission line flux in units of $10^{-8} \text{ erg s}^{-1} \text{ cm}^{-2}$, E_{obs} is the line energy, W_0 is the equivalent width, F_{DT13} is the flux measured by DT13, and W_{DT13} is their equivalent width. Errors are 90% confidence limits for a single parameter. *p* indicates a pegged limit.

^a Unconstrained or poorly constrained by the HETGS data. Required to be within the 90% confidence limits of DT13.

^b Attributed to calibration effects in CC mode.

disk temperature of $1.77 \pm 0.03 \text{ keV}$ and a 2–10 keV flux of $5.2 \times 10^{-8} \text{ erg s}^{-1} \text{ cm}^{-2}$. In contrast, in January we measure a disk temperature of $T_{\text{max}} = 1.33 \pm 0.01 \text{ keV}$ and an unabsorbed 2–9 keV flux of $1.1 \times 10^{-8} \text{ erg s}^{-1} \text{ cm}^{-2}$. For a distance of 10 kpc, this flux corresponds to an unabsorbed luminosity of $\sim 1.3 \times 10^{38} \text{ erg s}^{-1}$. Our best fit is shown in red in the left panel of Figure 2.

To search for relativistic lines in our HETGS spectra, we add three Gaussian emission lines to our fit model. We constrain the line energies and widths to be within the 90% confidence limits reported by DT13: the energies are $4.04 \pm 0.1 \text{ keV}$, $7.28 \pm 0.04 \text{ keV}$, and $8.14 \pm 0.16 \text{ keV}$, and the line width is $0.17 \pm 0.05 \text{ keV}$. In Figure 2, we show these emission lines at the fluxes reported by DT13 (blue curve). In our analysis we allow these fluxes to vary, but none are significant at the 3σ level. Indeed, we find that relative to the second observation of DT13, the flux in the redshifted and blueshifted Fe XXVI lines is reduced by factors of $\gtrsim 10$ and $\gtrsim 20$, respectively. The blueshifted Ni XXVII line is poorly constrained because of absorption lines in the HETGS spectrum (Figure 2, left).

3.2. 2012 June

In contrast to the pure disk continuum in January, we find a significant power law component in June, which we model using `simpl \otimes ezdiskbb` (Steiner et al. 2009). The asymptotic photon index is $\Gamma = 2.9^{+0.2}_{-0.3}$, but the fraction of scattered disk photons is unconstrained because of the low disk temperature ($T_{\text{max}} < 0.3 \text{ keV}$). The unabsorbed 2–9 keV flux is $1.4 \times 10^{-8} \text{ erg s}^{-1} \text{ cm}^{-2}$. We search for relativistic lines using the same procedure as above. Again we find no statistically-significant blueshifted emission¹ (Table 1). There is a feature detected near $\sim 4 \text{ keV}$, but with significant calibration uncertainties in CC mode associated with high column densities and bright/hard spectra, and no blueshifted counterpart, we believe it may be unphysical and does not support a June baryonic jet. We also note that the associated radio emission is optically thick, so the jet physics likely differs somewhat from that in DT13.

4. DISCUSSION

In their second *XMM-Newton*/ATCA observation of 4U 1630–47 in 2012 September, DT13 discovered rel-

ativistically Doppler-shifted Fe and Ni emission lines whose appearance coincided with steep-spectrum radio emission. But despite the $\sim 5\times$ brighter steep-spectrum radio emission during our ATCA observations in 2012 January, we found no evidence for the emission lines in our contemporaneous *Chandra* observations. With a tight upper limit on the blueshifted Fe XXVI emission line flux (it must have been $\gtrsim 20\times$ fainter than reported by DT13 eight months later), what can be said about the evolution of the baryon content of the jet in 4U 1630–47? What is the significance of *Chandra*’s non-detection of blueshifted emission lines?

Here we will focus on our January campaign, since it provides the strongest constraints. We can explain the absence of the lines in light of two scenarios: (1) there were relativistic baryons in the jet at the time of our campaign, but their X-ray emission was negligible, or (2) there were no relativistic baryons in the jet. Of course there is middle ground, but these scenarios span the plausible range of explanations. Below, we consider them in turn. In Section 4.3 we also discuss the association between the radio emission and relativistic lines seen by DT13.

4.1. 2012 January: Baryons but No Emission Lines

First, we suppose that despite the non-detection of baryonic emission during our *Chandra*/ATCA campaign, the jet had the same baryon content as in the *XMM*/ATCA observations. Specifically, we assume the jet emission mechanisms were the same (but see Section 4.3), and we consider either the jet baryon number density n_b or the total number of jet baryons N_b to be fixed. These considerations are reasonable in context because DT13 modeled the baryonic emission in their *XMM* spectrum as a 21 keV thermal plasma, for which the model normalization K is proportional to $\int n_e n_H dV \sim n_b N_b$; n_e is the electron density, n_H is the density of hydrogen, and the integral is over the emitting volume dV .

To suppress the plasma emission by ~ 20 , we can therefore invoke a smaller baryon density or a reduced number of baryons in the jet. Keeping N_b fixed and reducing n_b would require a $\sim 20\times$ larger jet, while keeping n_b fixed and reducing the total number of baryons would require a $\sim 20\times$ smaller jet. Physically, these scenarios could represent a jet at a different stage of formation. In either case (n_b or N_b fixed), some fine tuning of the plasma parameters would also be needed, since the optically thin

¹ There is a small residual near 7.3 keV (Figure 2), but an F-test indicates that it is not significant at the 90% confidence level.

synchrotron emission from the jet is sensitive to both the volume and the electron density in the emitting region.

Alternatively, we might explain the non-detection of the iron emission line by invoking a variation in the plasma temperature that significantly reduces the abundance of Fe XXVI and its emissivity. However, we can effectively rule out such a temperature variation by querying the APEC database that underlies the *bvapec* model used by DT13: the emissivity of Fe XXVI drops to 5% of its value at temperatures (1) below ~ 3 keV, where emission from Fe XXV would have been even more apparent, and (2) well above 100 keV, which would be difficult to reconcile with our cooler accretion disk and no apparent power law component in the X-ray spectrum. As noted in DT13, extreme line broadening could also effectively hide such lines, but the iron line would need to be nearly an order of magnitude broader to be undetectable with *Chandra*, and it is difficult to explain such a large change in the expansion speed of the jet.

4.2. 2012 January: No Baryons

Perhaps the simplest interpretation is the one that takes our data at face value: we did not observe relativistic iron emission lines with *Chandra* because there were no baryons in the 2012 January jet. In this interpretation, the question is not why we did not observe the relativistic emission lines, but why DT13 did. What changed in the accretion flow between our campaign and theirs (and, for that matter, between their two reported *XMM* observations)?

The most significant difference in the observations appears to be the accretion state. As noted above, the X-ray luminosity of 4U 1630–47 in the second *XMM* observation was $\sim 3 - 5\times$ higher than in January and June. Notably, that luminosity corresponds to a significant fraction ($\sim 50\%$) of the Eddington luminosity for a $10 M_{\odot}$ black hole at a distance of 10 kpc, and $\gtrsim 50\%$ of the emission was in a hard power law. These facts raise the possibility that the stronger, brighter non-thermal component, the very high accretion power, or the extreme luminosity of the source may have played a role in lifting and/or helping to accelerate heavy particles.

4.3. 2012 September: Jet-ISM Interaction?

It is also worth considering whether or not the relativistic emission lines are indicative of baryonic matter in a relativistic jet, or if they can truly be associated with the radio emission at all. The primary reasons for this are that radio jets have been somewhat elusive in 4U 1630–47 (Tomsick et al. 2005), and our ATCA detections in January are atypical for steady jets from stellar-mass black holes. As mentioned in Section 2.2, our radio light curve looks like a faint, optically thin flare that lasts many weeks. Since our initial ATCA detections of very faint optically thin emission occur ~ 50 days after a major hard-soft state transition (Fig. 1; MJD $\sim 55900 - 55910$), and in what appears to be a standard disk-dominated state, we are inclined to interpret them as indicative of a jet-ISM interaction far from the black hole. See Fender et al. (2009) and references therein for a thorough discussion of similar detections in spectrally soft states.

Given the similar optically-thin spectrum, could the 2012 September 28 radio emission also originate in a

jet-ISM interaction? Inspection of the light curves and hardness-intensity diagram in Figure 1 reveals that between June and September there was a transition from a spectrally hard state to a softer state, although the date is difficult to identify precisely. Such transitions are usually associated with a transient ejection, and the optically thick radio emission in June might indicate the start of radio flaring periods typical of these transitions. If the associated ejection reached the ISM 2 – 4 months later, it could potentially explain the radio emission in the second *XMM*/ATCA observation. If that is the case, then the relativistic lines might not have been associated with the radio source at all, i.e., the radio emission could have been produced in the nearby ISM, while the X-ray lines were local to 4U 1630–47. For example, at a temperature of 21 keV, a relativistic wind would appear in emission in front of the accretion disk, although some obscuration, absorption, or geometrical effects might be needed to explain the line profiles.

However, we cannot say for certain that the radio emission mechanism was the same in January and September, so the possibility remains that we observed a jet-ISM interaction early in the outburst and DT13 observed a baryon-loaded jet later in the outburst. It may be possible to test these interpretations with future observations of that luminous second state. Regardless, it is clear that the observations from 2012 trace a complex relationship between the physics of the radio jet and the X-ray spectrum in 4U 1630–47.

5. CONCLUSION

The baryon content of astrophysical jets has important consequences for our understanding of their formation and their effects on their environment, but it is difficult to measure directly. Díaz Trigo et al. (2013) have argued that their detection of relativistically Doppler-shifted emission lines in 4U 1630–47 in September 2012 (MJD 56181) implies the presence of a baryonic jet, most likely launched from the rotating accretion disk (Blandford & Payne 1982). We cannot directly test this interpretation, but in this paper we have used *Chandra* HETGS observations from earlier in the same outburst (January/June, MJD $\sim 55954/56081$) to demonstrate that radio emission in 4U 1630–47 is not always associated with relativistic X-ray emission lines. The unique behavior observed with *XMM-Newton* and ATCA later in the outburst may be a special case, dependent on additional processes in the accretion flow around the black hole. However, because much of the observed radio emission from 4U 1630–47 in 2012 is consistent with jet-ISM interactions, we cannot rule out scenarios where the X-ray emission lines originate in a hot outflow that is not physically related to the radio source. Further analysis of the X-ray and radio emission (Neilsen et al., in preparation) may help test our interpretation of this exciting physics.

We thank the referee for constructive comments. J.N. acknowledges funding from NASA through the Einstein Postdoctoral Fellowship, grant PF2-130097, awarded by the CXC, which is operated by the SAO for NASA under contract NAS8-03060. GP acknowledges support via an EU Marie Curie Intra-European Fellowship under contract no. FP7-PEOPLE-2012-IEF-331095. We thank N.

Schulz and D. Huenmoerder for advice regarding plasma models. ATCA is part of the Australia Telescope National Facility which is funded by the Commonwealth of

Australia for operation as a National Facility managed by CSIRO.

REFERENCES

- Baganoff, F. K., Maeda, Y., Morris, M., et al. 2003, *ApJ*, 591, 891
 Blandford, R. D., & Payne, D. G. 1982, *MNRAS*, 199, 883
 Blandford, R. D., & Znajek, R. L. 1977, *MNRAS*, 179, 433
 Canizares, C. R., Davis, J. E., Dewey, D., et al. 2005, *PASP*, 117, 1144
 Carrasco-González, C., Rodríguez, L. F., Anglada, G., et al. 2010, *Science*, 330, 1209
 Davis, J. E. 2001, *ApJ*, 562, 575
 Díaz Trigo, M., Miller-Jones, J. C. A., Migliari, S., Broderick, J. W., & Tzioumis, T. 2013, *Nature*, 504, 260
 Fabian, A. C., Sanders, J. S., Etori, S., et al. 2000, *MNRAS*, 318, L65
 Fender, R. P., Belloni, T. M., & Gallo, E. 2004, *MNRAS*, 355, 1105
 Fender, R. P., Gallo, E., & Russell, D. 2010, *MNRAS*, 406, 1425
 Fender, R. P., Garrington, S. T., McKay, D. J., et al. 1999, *MNRAS*, 304, 865
 Fender, R. P., Homan, J., & Belloni, T. M. 2009, *MNRAS*, 396, 1370
 Gallo, E., Fender, R., Kaiser, C., et al. 2005, *Nature*, 436, 819
 Heinz, S. 2006, *ApJ*, 636, 316
 Houck, J. C., & Denicola, L. A. 2000, in *ASP Conf. Ser.*, Vol. 216, *Astronomical Data Analysis Software and Systems IX*, ed. N. Manset, C. Veillet, & D. Crabtree (San Francisco, CA: ASP), 591
 Jones, C., Forman, W., Tananbaum, H., & Turner, M. J. L. 1976, *ApJ*, 210, L9
 King, A. L., Miller, J. M., Gültekin, K., et al. 2013a, *ApJ*, 771, 84
 King, A. L., Miller, J. M., Raymond, J., et al. 2013b, *ApJ*, 762, 103
 King, A. L., Walton, D. J., Miller, J. M., et al. 2014, *ArXiv e-prints*, arXiv:1401.3646
 Kuulkers, E., Parmar, A. N., Kitamoto, S., Cominsky, L. R., & Sood, R. K. 1997, *MNRAS*, 291, 81
 McNamara, B. R., Wise, M., Nulsen, P. E. J., et al. 2000, *ApJ*, 534, L135
 Miller, J. M., Raymond, J., Reynolds, C. S., et al. 2008, *ApJ*, 680, 1359
 Narayan, R., & McClintock, J. E. 2012, *MNRAS*, 419, L69
 Neilsen, J. 2013, *Advances in Space Research*, 52, 732
 Neilsen, J., & Homan, J. 2012, *ApJ*, 750, 27
 Neilsen, J., & Lee, J. C. 2009, *Nature*, 458, 481
 Neilsen, J., Remillard, R. A., & Lee, J. C. 2011, *ApJ*, 737, 69
 Nowak, M. A., Neilsen, J., Markoff, S. B., et al. 2012, *ApJ*, 759, 95
 Ponti, G., Fender, R. P., Begelman, M. C., et al. 2012, *MNRAS*, 422, L11
 Punsly, B., & Rodriguez, J. 2013, *MNRAS*, 435, 2322
 Russell, D. M., Gallo, E., & Fender, R. P. 2013, *MNRAS*, 431, 405
 Sault, R. J., Teuben, P. J., & Wright, M. C. H. 1995, in *ASP Conf. Ser.*, Vol. 77, *Astronomical Data Analysis Software and Systems IV*, ed. R. A. Shaw, H. E. Payne, & J. J. E. Hayes, 433
 Steiner, J. F., McClintock, J. E., & Narayan, R. 2013, *ApJ*, 762, 104
 Steiner, J. F., Narayan, R., McClintock, J. E., & Ebisawa, K. 2009, *PASP*, 121, 1279
 Tchekhovskoy, A., Narayan, R., & McKinney, J. C. 2011, *MNRAS*, 418, L79
 Tomsick, J. A., Corbel, S., Goldwurm, A., & Kaaret, P. 2005, *ApJ*, 630, 413
 Verner, D. A., Ferland, G. J., Korista, K. T., & Yakovlev, D. G. 1996, *ApJ*, 465, 487
 Wilms, J., Allen, A., & McCray, R. 2000, *ApJ*, 542, 914
 Wilson, W. E., Ferris, R. H., Axtens, P., et al. 2011, *MNRAS*, 416, 832
 Zimmerman, E. R., Narayan, R., McClintock, J. E., & Miller, J. M. 2005, *ApJ*, 618, 832